Supporting Information

Switchable Supramolecular Polymers of Pt(II) Complex via Diacetylene π–Ag^+ Interaction

Yumi Park,[a] Woomin Jeong,[b] Kayoung Kim,[c] Jong-Man Kim [b] and Jong Hwa Jung [*a,c]

[a.] *Department of Chemistry, Gyeongsang National University (GNU)*
Jinju 52828, Republic of Korea
[b.] *Department of Chemical Engineering, Hanyang University*
Seoul 04763, Republic of Korea
[c.] *Technical Support Center for Chemical Industry, Korea Research Institute of Chemical Technology (KRICT)*
Ulsan 44429, Republic of Korea
[d.] *Research Institute of Advanced Chemistry, Gyeongsang National University (GNU)*
Jinju 52828, Republic of Korea
E-mail: jonghwa@gnu.ac.kr

Table of Contents

1. General

1.1 General Characterization

The ^{1}H and ^{13}C NMR spectra were taken on a Bruker DRX 300 and a Bruker DRX 400. The high-resolution mass spectra (HR-MS) were measured by electrospray ionization (ESI) with a micro TOF Focus spectrometer from SYNAPT G2 (Waters, U.K.). IR spectra were observed over the range 500-4000 cm^{-1}, with a Thermo Scientific Nicolet iS 10 model.

1.2 Atomic Force Microscopy (AFM) Studies

Atomic force microscope (AFM) imaging was performed by using XE-100 and a PPP-NCHR 10 M cantilever (Park systems). The AFM samples were prepared by spin-coating (2000 rpm) onto freshly cleaved Muscovite Mica, and images were recorded with the AFM operating in a noncontact mode in the air at RT with a resolution of 1024 × 1024 pixels, using moderate scan rates (0.3 Hz).

1.3 PL Studies

The photoluminescence (PL) spectra were recorded on a JASCO FP-8650 fluorescence spectrophotometer. The PL spectra were measured over the range of 450-750 nm using a quartz cell with a 2 mm path length. Scans were taken at a rate of 400 nm/min with a sampling interval of 1 nm and a response time of 1 s. To investigate the supramolecular polymerization process, temperature- and time-dependent PL spectral changes were monitored with an excitation wavelength of 400 nm.

1.4 UV-vis Studies

The UV-vis spectra were recorded on a Jasco V-750 UV spectrophotometer. The UV-vis spectra were determined over the range of 250-500 nm using a quartz cell with 2 mm path lengths. Scans were taken at a rate of 1000 nm/min with a sampling interval of 1 nm and a response time of 1 s. To elucidate the supramolecular polymerization process, it was heated to 363 K (1 K/min) to form the monomeric species in UV-vis spectroscopy. Then the sample was cooled to 293 K (1 K/min) in UV-vis spectroscopy. The time-dependent UV-vis spectral changes were measured at 293 K.

1.5 Thermodynamic Studies

The molar fraction of aggregated molecules (α_{agg}) at a certain temperature was calculated from the absorbance at 564 nm in which Abs(agg) and Abs(mono) are the absorption intensities of fully aggregated (at the lowest temperature) and purely monomeric states (at the highest temperature), respectively, and Abs(T) is the absorption intensity at a given temperature (T). [1]

$$\alpha_{agg} = 1 - \frac{Abs(agg) - Abs(T)}{Abs(agg) - Abs(mono)}$$

The plot of α_{agg} versus temperature provides heating curves with non-sigmoidal (cooperative mechanism) shapes, which were fitted using the models proposed by Meijer *et al*.[2] (for

cooperative mechanism). The standard values of enthalpy (Δ*H*°), entropy (Δ*S*°), and Gibbs free energy (Δ*G*°) were calculated using the van't Hoff equation. The van't Hoff plots were produced using an equation by a method that has been proposed in previous literature.[3] The values for the entropy change (Δ*S*) and enthalpy change (Δ*H*) as used in the cooperative supramolecular polymerization models were obtained by fitting to the heating curves.[4-6] These heating curves were obtained by temperature-dependent UV-vis spectra.

1.6 Fitting of Heating Curves

Cooperative fits were performed using MATLAB R2008b software. Though the codes pertain to one component system, we have extrapolated them to two-component systems, and the thermodynamic parameters thus obtained are well within accepted limits.[7]

1.7 Preparation of Silver(I) Complexes

Pt_2L^1 (100 µM) was dissolved in DMSO. $AgNO_3$ (1-3.0 equivalent) was dissolved in H_2O. The **Pt_2L^1** solution was added to $AgNO_3$ (1-3.0 equivalent) solution. The mixed solvent ratio was maintained at DMSO/H_2O (3:7 v/v).

1.8 DFT Calculation

We performed density functional theory (DFT) calculations to optimize the ligands **Pt_2L^1** using the Gaussian 09 package.[8] The unrestricted B3LYP functional was employed for all optimizations and frequency calculations with 3-21G level of theory for all atoms.[9-11] All calculations were performed in the gas phase.

2. Synthesis and Characterization

Unless otherwise noted, chemical reagents and solvents were purchased from commercial suppliers (Tokyo Chemical Industry (TCI), Sigma Aldrich) and used without further purification.

2.1 Synthesis of 1

In a two-neck flask, the solution of 4-pentyn-1-ol (2.58 mL, 23.8 mmol) in acetonitrile were added CuCl(I) (0.24 g, 2.38 mmol) and *N,N,N',N'*-Tetramethylethylenediamine (TMEDA) (1.07 mL 7.13 mmol). Oxygen was bubbled in the solution and stirred for 3 h at room temperature. After completion of reaction, the reaction mixture was filtered. The filtrate was dried under reduced pressure. The crude material was purified by column chromatography (40% EA in Hexane) to give a white crystalline solid **1** in 93.6% yield (1.85 g). IR (ATR): 3247, 3162, 2935, 2854, 2148, 1427, 1330, 1280, 1168, 1045, 902, 740 cm^{-1}; ^1H NMR (300 MHz, $CDCl_3$): δ 3.74 (t, 4H), 2.38 (t, 4H), 1.77 (p, 4H); ^{13}C NMR (400 MHz, $CDCl_3$): δ 76.84, 65.63, 61.34, 30.94, 15.72; HR-Mass (m/z) calculated for $C_{10}H_{14}O_2$ $[M]^+$: 166.0988, Found $[M+Na]^+$: 189.0886.

2.2 Synthesis of 2

A *Jones reagent* was prepared by addition of H_2SO_4 (3.45 mL, 64.38 mmol) in water to an aqueous solution of chromium trioxide (4.52 g, 45.14 mmol) at 0 °C. The *Jones reagent* was

then added dropwise to an acetone solution of **1** (1.5 g, 9.02 mmol) and the solution was stirred for 3 h at room temperature. The reaction mixture was quenched with 2-propanol and insoluble solid was removed by filtration. The filtrate was dried and dissolved again in chloroform. The crude material was filtered, washed with chloroform and diethyl ether and dried under reduced pressure to obtain desired product and got a white solid **2** in 49.1% yield (0.86 g). IR (ATR): 3023, 2919, 2857, 2626, 1685, 1423, 1292, 1207, 921, 775, 682 cm^{-1}; ^{1}H NMR (300 MHz, DMSO-d_6): δ 12.3 (s, 2H), 2.47 (d, 2H), 2.43 (t, 2H); ^{13}C NMR (400 MHz, DMSO-d_6): δ 173.11, 77.72, 65.65, 63.29, 32.93, 32.71, 29.43, 27.40, 15.66, 14.96; HR-Mass (m/z) calculated for $C_{10}H_{10}O_4$ $[M]^+$: 194.0574, Found $[M+Na]^+$: 217.0471.

2.3 Synthesis of 3

(*R*)-(−)-2-amino-1-propanol (0.28 g, 3.7 mmol) was added to a stirred suspension of powdered KOH (1.05 g, 18.7 mmol) in dry DMSO (20 mL) at 60 °C. After 30 min, 4′-chloro-2,2′:6′,2″-terpyridine (1.00 g, 3.7 mmol) was added to the mixture. The mixture was then stirred for 4 h at 70 °C and poured into 600 mL of distilled water thereafter. CH_2Cl_2 (3 × 200 mL) was used to extract the aqueous phase. Residual water in dichloromethane was dried over Na_2SO_4 and CH_2Cl_2 was removed in a vacuum, and the desired product was purified by recrystallization with ethyl acetate to give 0.72 g (72%) of **3**. Mp = 118.3 °C; IR (ATR): 3375, 2964, 2926, 2846, 1577, 1565, 1473, 1439, 1403, 1353, 1204, 799 cm^{-1}; ^{1}H NMR (300 MHz, $CDCl_3$): δ 8.70 (tdd, *J* = 4.8, 1.8, 0.9 Hz, 2H), 8.62 (dt, *J* = 8.0, 1.1 Hz, 2H), 8.02 (s, 2H), 7.84 (td, *J* = 7.7, 1.8 Hz, 2H), 7.33 (ddd, *J* = 7.4, 4.8, 1.2 Hz, 2H), 4.14 (dd, *J* = 9.0, 4.1 Hz, 1H), 3.94 (dd, *J* = 9.1, 7.6 Hz, 1H), 3.41 (dddd, *J* = 10.6, 7.6, 6.6, 4.2 Hz, 1H), 1.21 (d, *J* = 6.5 Hz, 3H); ^{13}C NMR (125 MHz, DMSO-d_6): δ 167.2, 157.1, 155.3, 149.7, 137.9, 125.0, 121.3, 107.3, 75.1, 46.2, 20.43; HR-Mass (m/z) calculated for $C_{18}H_{18}N_4O$ $[M]^+$: 306.1475, Found $[M+H]^+$: 307.2561.

2.4 Synthesis of 4

To a solution of **2** in DMF, was added **3**, followed by addition of N-(3-dimethylaminopropyl)-N′-ethylcarbodiimide hydrochloride (0.296 g, 1.54 mmol), 1-hydroxybenzotriazole hydrate (0.063 g, 0.46 mmol) and sodium bicarbonate (0.104, 1.24 mmol). The resulting solution was stirred for 2 days at room temperature under N_2. After completion of reaction, the solvent was evaporated, the residue was extracted with chloroform and brine. The organic phase was dried with $MgSO_4$ and dried under reduced pressure. The desired product was recrystallized from ethyl acetate and got a pink solid **4** in 60.2% yield (0.239 g). IR (ATR): 3286, 3054, 2919, 2857, 1731, 1639, 1558, 1446, 1403, 1357, 1245, 1195, 1033, 323, 867, 790, 732 cm^{-1}; ^{1}H NMR (300 MHz, $CDCl_3$): δ 8.68 (d, 4H), 8.58 (d, 4H), 8.00 (s, 4H), 7.84 (td, 4H), 7.33 (ddd, 4H), 4.46 (dt, 4H), 4.22 (dd, 4H), 4.16 (s, 4H), 2.52 (t, 4H), 2.30 (t, 4H), 1.33 (d, 6H); ^{13}C NMR (400 MHz, $CDCl_3$): δ 170.28, 167.28, 148.72, 124.26, 121.69, 107.76, 76.14, 71.04, 66.10, 44.57, 35.02, 29.72, 17.50, 15.68; HR-Mass (m/z) calculated for $C_{46}H_{42}N_8O_4$ $[M]^+$: 770.3324, Found $[M+Na]^+$: 793.3321.

2.5 Synthesis of Pt_2L^1

L^1 (0.15048 g) was added and dried under vacuum. Methanol (20 mL) was added, and the mixture was heated to 90 °C until the solid completely dissolved. Dichloro(1,5-

cyclooctadiene)platinum(II) (0.1459 g) was added to the solution. After completion of reaction, the solvent was removed under reduced pressure. The crude product was purified by recrystallization from methanol/diethyl ether to give 52.4% yield (0.632 g). IR (ATR): 3367, 3232, 3050, 2915, 2854, 2345, 2105, 1735, 1646, 1608, 1554, 1465, 1427, 1357, 1218, 1172, 1103, 1037, 867, 786, 709cm^{-1}; ^{1}H NMR (300 MHz, DMSO-d_6): δ 8.47 (d, 4H), 8.38 (m, 4H), 8.08 (s, 2H), 7.81 (t, 2H), 7.70 (m, 1H), 4.21 (s, 2H), 4.10 (d, 2H), 2.57 (d, 4H), 2.42 (d, 4H), 1.26 (m, 8H), 0.81 (m, 6H); ^{13}C NMR (400 MHz, DMSO-d_6): δ 170.82, 158.25, 155.53, 151.40, 142.75, 129.68, 126.30, 111.61, 78.33, 73.69, 66.04, 44.30, 41.29, 40.78, 40.57, 40.37, 40.16, 40.08, 39.95, 39.44, 17.47, 15.43; HR-Mass (m/z) calculated for $C_{46}H_{42}N_8O_4Pt_2Cl_2$ $[M]^+$: 1229.1975, Found $[M+Na]^+$: 1252.1873.

2.6 Synthesis of Pt_2L^2

Pt_2L^2 was synthesized according to reports published previously. Spectral data were the same as reported previously.[12]

3. Supplementary Figures

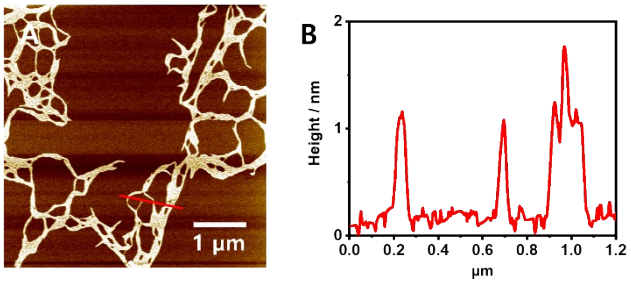

Fig. S1 AFM image and heigh profile of the SP derived from **Pt_2L^1** in a mixed DMSO and H_2O (3:7 v/v).

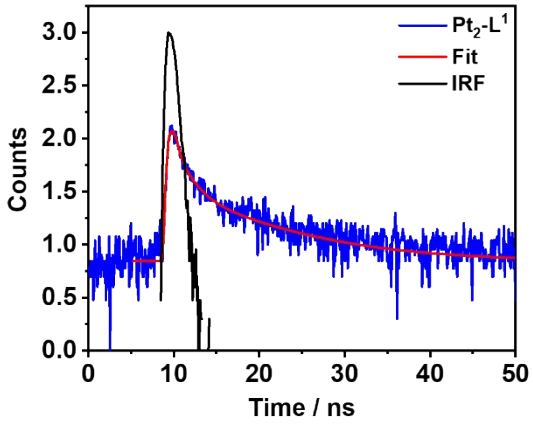

Fig. S2 Fluorescence lifetime of $\mathbf{Pt_2L^1}$ (50 μM) in DMSO/H_2O (3:7 v/v).

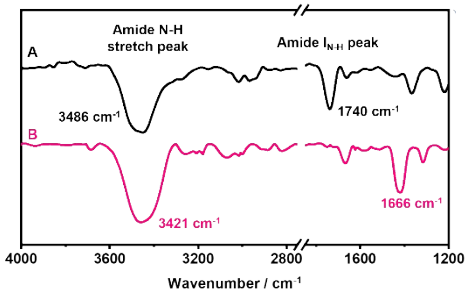

Fig. S3 FT-IR spectra of **Pt_2L^1** in (A) DMSO only (black line) and (B) DMSO and H_2O (3:7 v/v) (pink line).

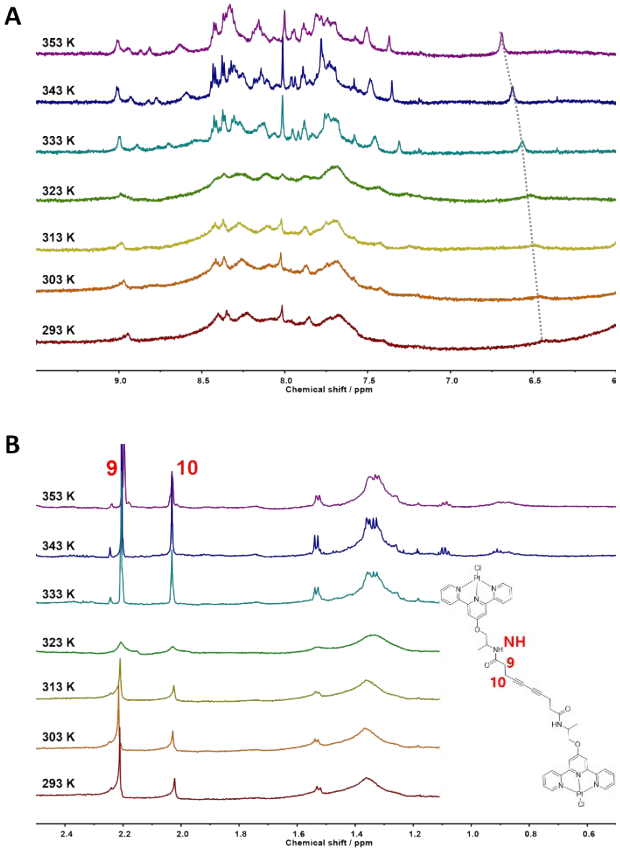

Fig. S4 Temperature dependent ^{1}H-NMR spectra of **Pt_2L^1** at (A) downfield (6~10 ppm) and (B) up-field (0.5~2.5 ppm) in DMSO-d_6 and D_2O (3:7 v/v) from 298 K to 353 K.

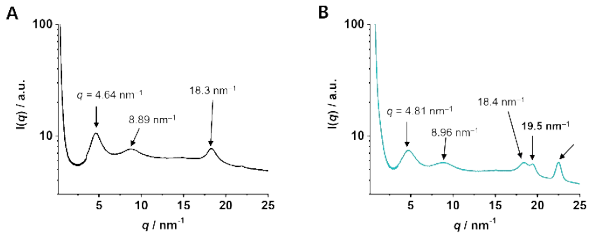

Fig. S5 XRD patterns of Pt_2L^1 in the (A) absence and (B) presence of $AgNO_3$ (2 equiv.).

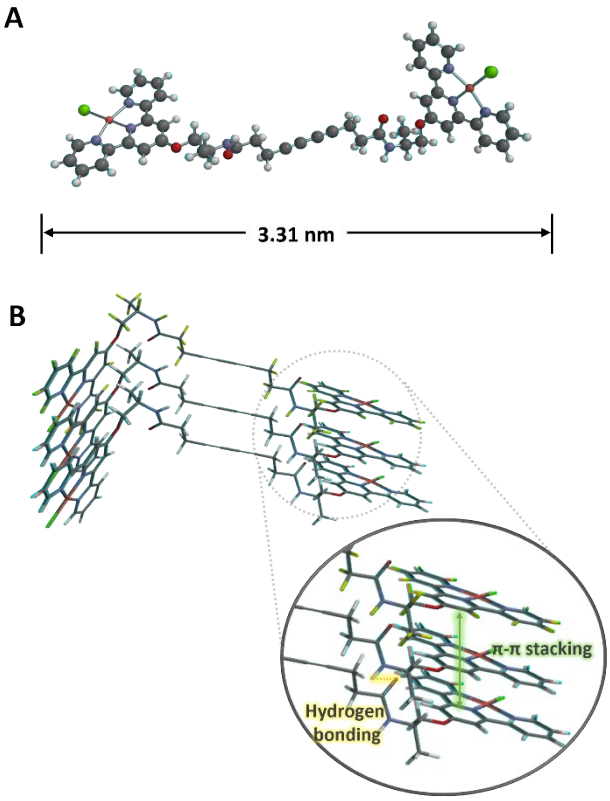

Fig. S6 Optimized (A) Pt_2L^1 and (B) proposed molecular stacking structure of Pt_2L^1 in supramolecular polymerization with intermolecular hydrogen bonding and π-π Stacking.

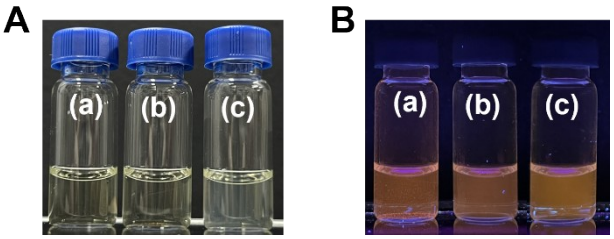

Fig. S7 Photographs under (A) ambient light and (B) UV light about (a) $\mathbf{Pt_2L^1}$ in the presence of $AgNO_3$ (b) 1 equiv. and (c) 2 equiv. in DMSO and H_2O (3:7 v/v).

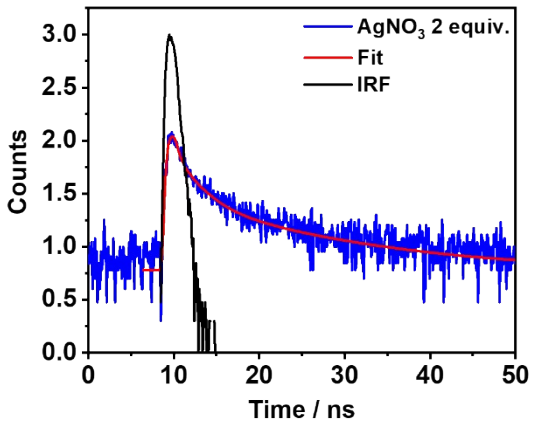

Fig. S8 Fluorescence lifetime about $\mathbf{Pt_2L^1}$ (100 μM) in the presence of $AgNO_3$ in DMSO and H_2O (3:7 v/v).

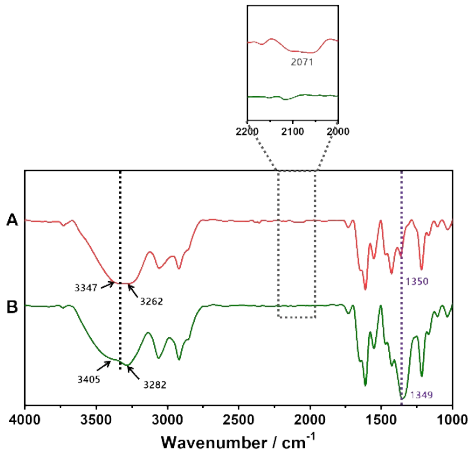

Fig. S9 FT-IR spectra of $\mathbf{Pt_2L^1}$ (200 µM) in the (A) absence (red line) and (B) presence (green line) of $AgNO_3$ (2 equiv.) in DMSO and H_2O (3:7 v/v, green line).

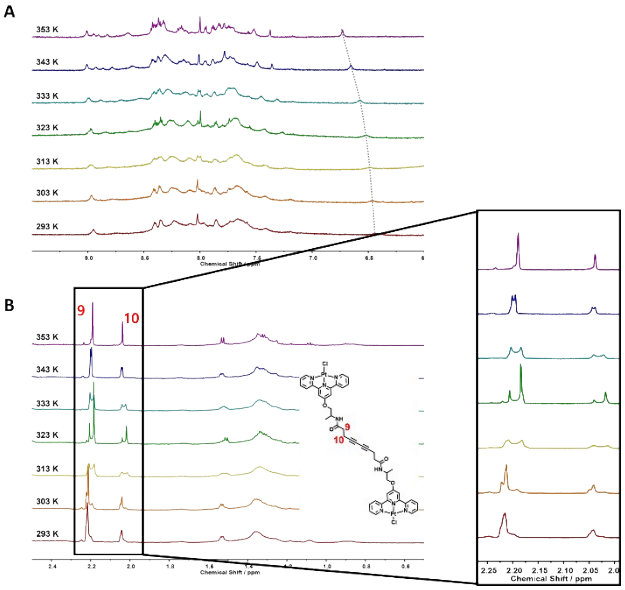

Figure S10. Temperature dependent ^{1}H-NMR spectra in presence of $AgNO_3$ to Pt_2L^1 at (A) downfield (6~10 ppm) and (B) upfield (0.5~2.5 ppm) in DMSO-d_6 and D_2O from 298 K to 353 K.

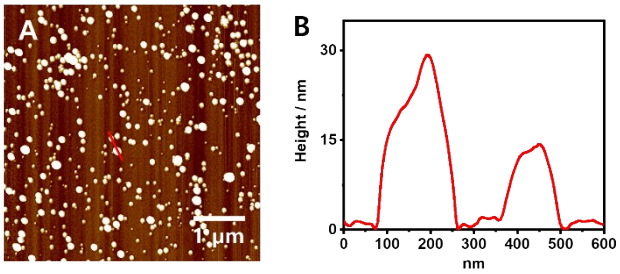

Fig. S11 (A) AFM image and (B) height profile of SP based on **Pt_2L^1** (100 μm) in the presence of $AgNO_3$ (2.0 equiv.) in DMSO and H_2O (3:7 v/v).

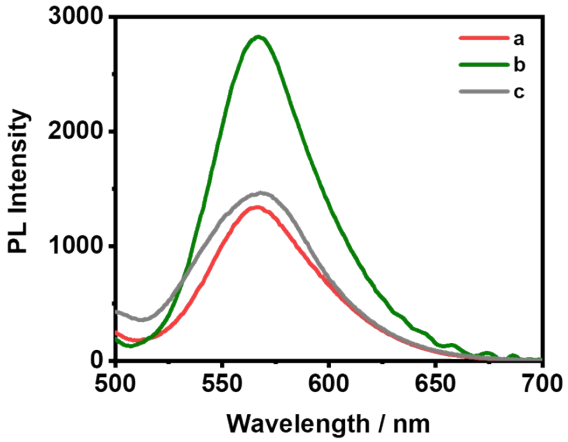

Fig. S12 PL spectra of (a) $\mathbf{Pt_2L^1}$ (100 μm) in (b) the presence of $AgNO_3$ (2.0 equiv.) upon addition of (c) NaCl (5.0 equiv.) in DMSO and H2O (3:7 v/v).

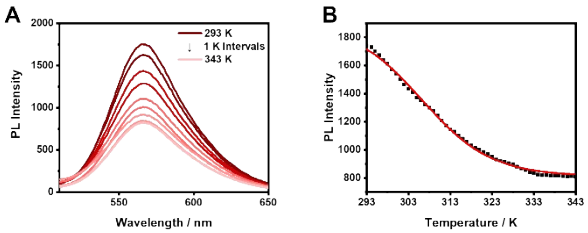

Fig. S13 (A) Temperature-dependent PL spectra and (B) Plots of PL Intensity at 564 nm about $\mathbf{Pt_2L^1}$ in the presence of $AgNO_3$ (2 equiv.) from 293 K to 343 K in DMSO/H_2O (v/v = 3:7).

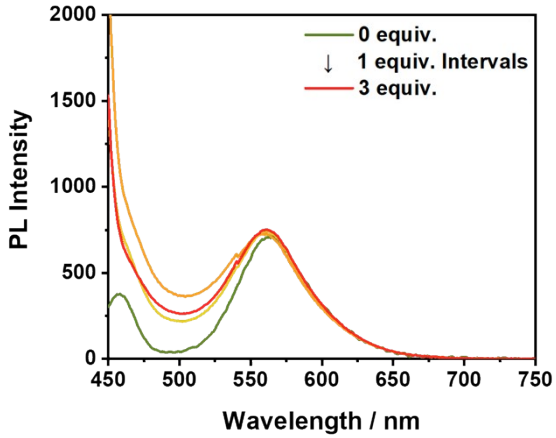

Fig. S14 PL spectra of $\mathbf{Pt_2L^2}$ (100 μM) in the presence of $AgNO_3$ (0~3 equiv.) in DMSO/H_2O (3:7 v/v).

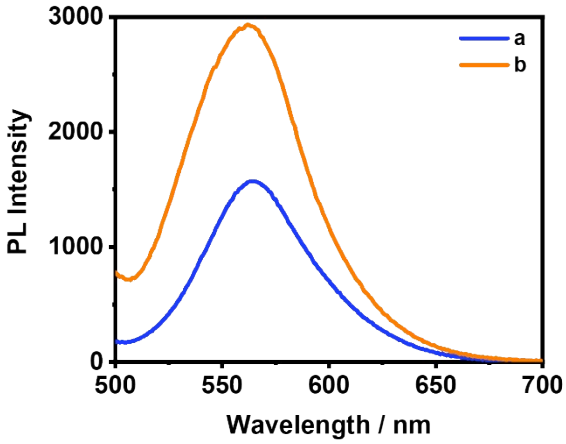

Fig. S15 PL spectra of **Pt_2-L^1** (100 μM) in the presence of $AgNO_3$ (2.0 equiv.), and **L^3** (5.0 equiv.), recorded (a) before and (b) after the addition of $Zn(NO_3)_2$ (10 equiv.) in DMSO/H_2O (3:7 v/v).

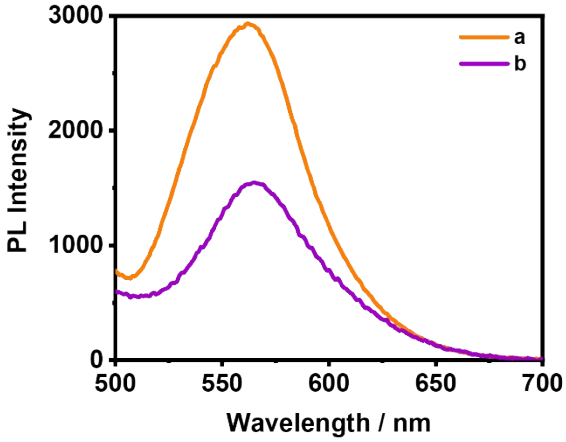

Fig. S16 PL spectra of **Pt_2-L^1** (100 μM) in the presence of $AgNO_3$ (2.0 equiv.), **L^3** (5.0 equiv.), and $Zn(NO_3)_2$ (10 equiv.), recorded (a) before and (b) after the addition of tetramethylammonium chloride (20 equiv.) in DMSO/H_2O (3:7 v/v).

Table S1. Thermodynamic parameters of (A) Pt_2L^1 and in the (B) presence of $AgNO_3$.

	A	B
ΔG (kJ mol^{-1})	-25.52	-27.57
ΔH_e (kJ mol^{-1})	-65.75	-106.88
ΔS (kJ mol^{-1} K^{-1})	-137.28	-270.66
ΔH_n (kJ mol^{-1})	-0.00	-0.00
T_e (K)	291.71	302.77
K_e (L mol^{-1})	3.55 x 10^4	8.24 x 10^4
σ	1	1
K_n	3.55 x 10^4	8.24 x 10^4

Table S2. Luminescence lifetimes of (A) Pt_2L^1 and in the (B) presence of $AgNO_3$.

	CHI	<Tau>	Tau1	Tau2	Tau3	A1	A2	Background
A	0.986637	8.00954	1.50235e-008	1.6461	10.186	162.043	4.15674	7
B	1.05342	9.5287	0.126375	2.54758	15.3265	53.7375	4.11215	6

4. Analytical Data

4.1 ^{1}H- and ^{13}C-NMR Spectoscopy

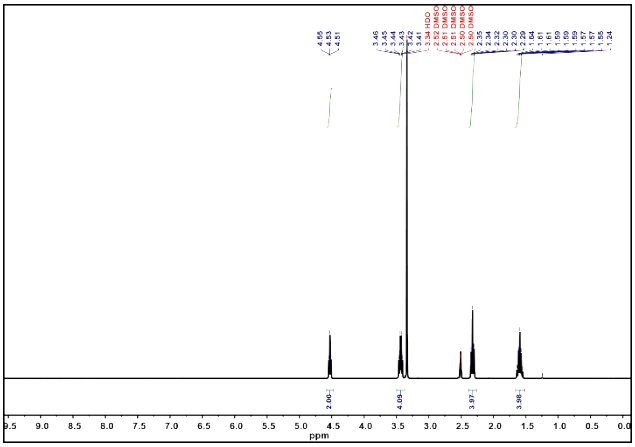

Fig. S17 ^{1}H NMR spectrum (300 MHz) of **1** in DMSO-d_6 at 25 °C.

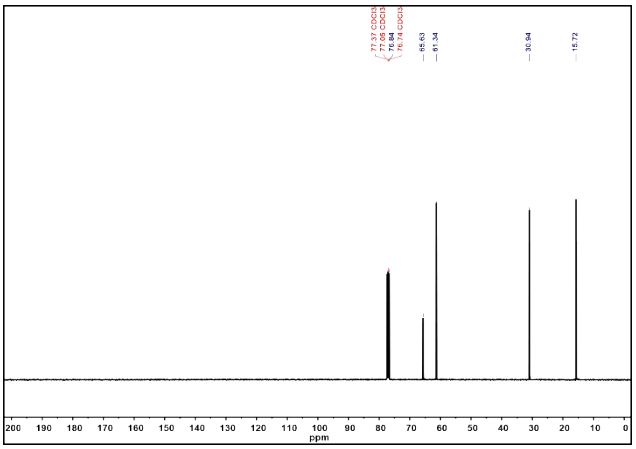

Fig. S18 ^{13}C NMR spectrum (300 MHz) of **1** in $CDCl_3$ at 25 °C.

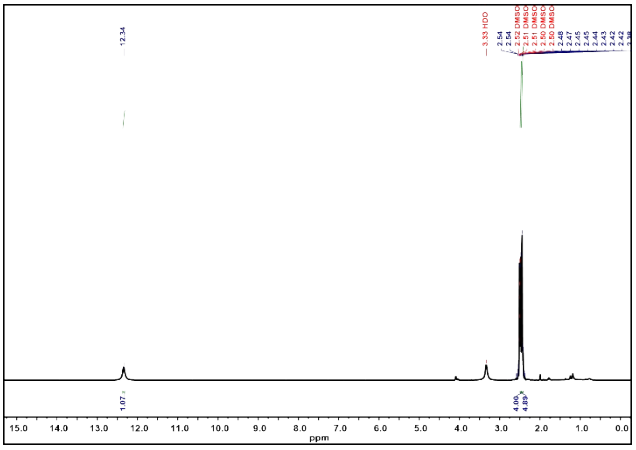

Fig. S19 ^{1}H NMR spectrum (300 MHz) of **2** in DMSO-d_6 at 25 °C

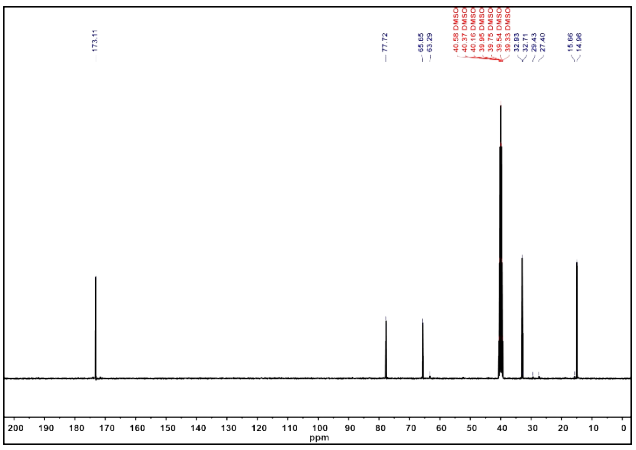

Fig. S20 ^{13}C NMR spectrum (300 MHz) of **2** in DMSO-d_6 at 25 °C.

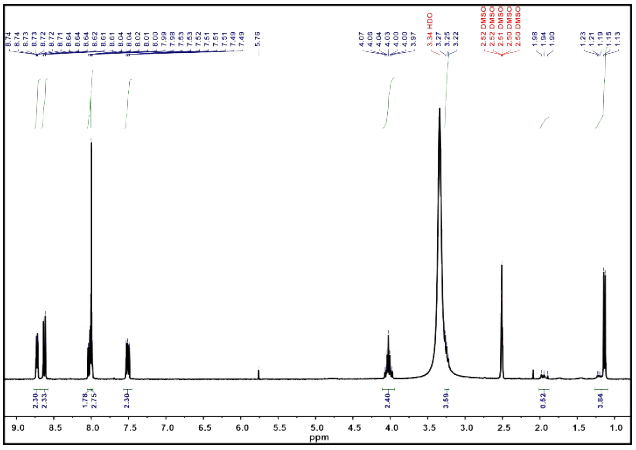

Fig. S21 ^{1}H NMR spectrum (300 MHz) of **3** in DMSO-d_6 at 25 °C.

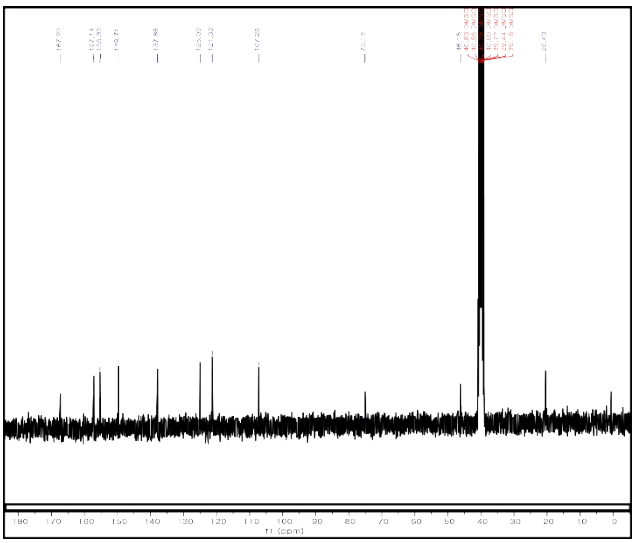

Fig. S22 ^{13}C NMR spectrum (75 MHz) of **3** in DMSO-d_6 at 25 °C.

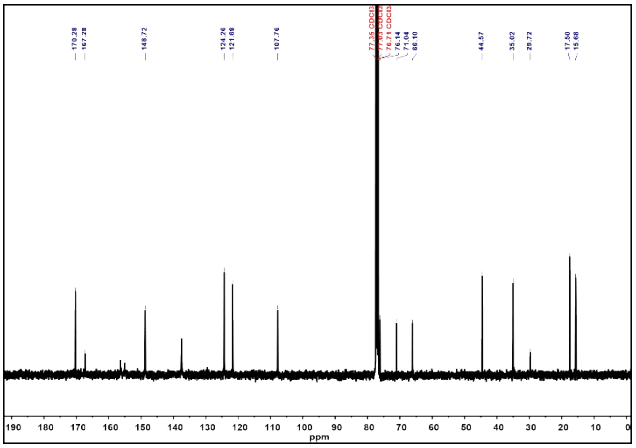

Fig. S23 ^{1}H NMR spectrum (300 MHz) of **4** in $CDCl_3$ at 25 °C.

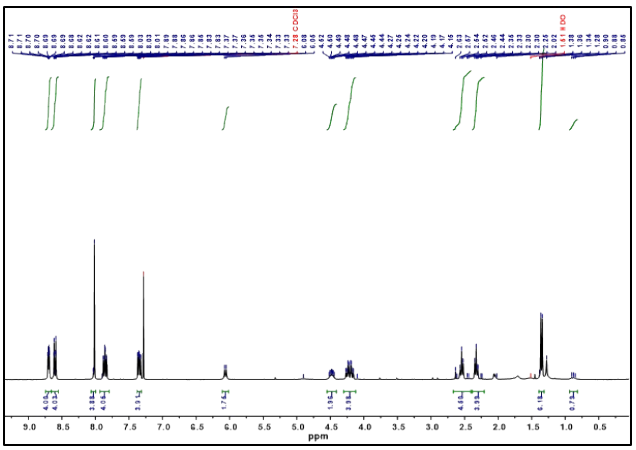

Fig. S24 ^{13}C NMR spectrum (300 MHz) of **4** in $CDCl_3$ at 25 °C.

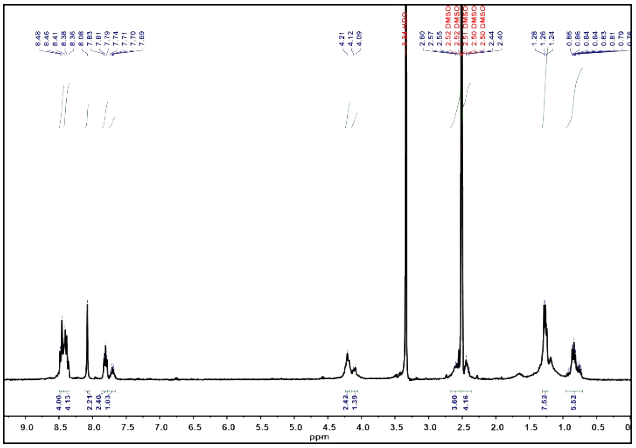

Fig. S25 ^{1}H NMR spectrum (300 MHz) of **Pt_2L^1** in DMSO-d_6 at 25 °C.

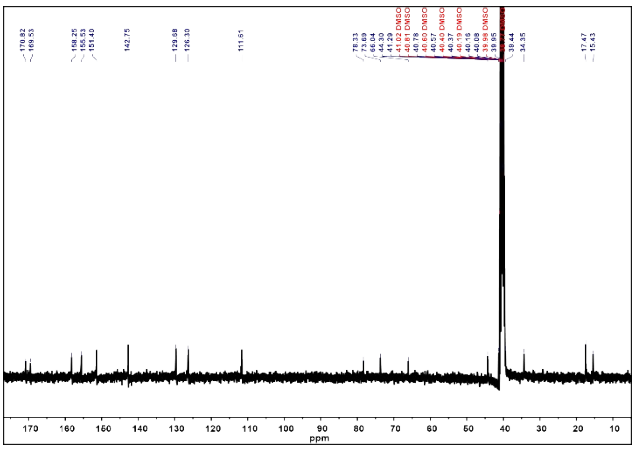

Fig. S26 ^{13}C NMR spectrum (300 MHz) of **Pt_2L^1** in DMSO-d_6 at 25 °C.

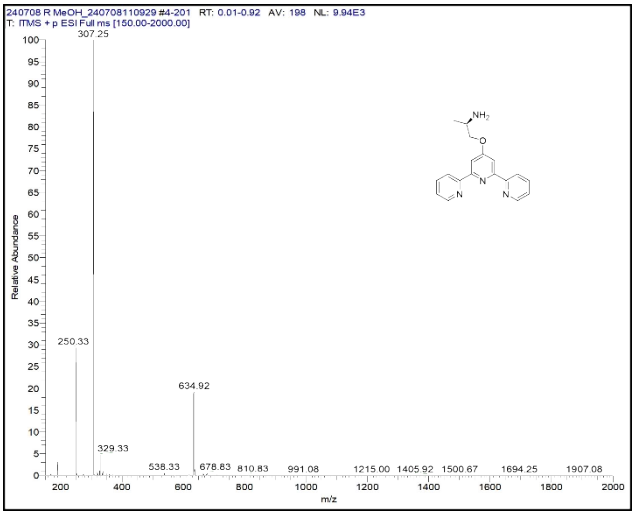

Fig. S27 ESI Mass spectrum of **3** in Methanol.

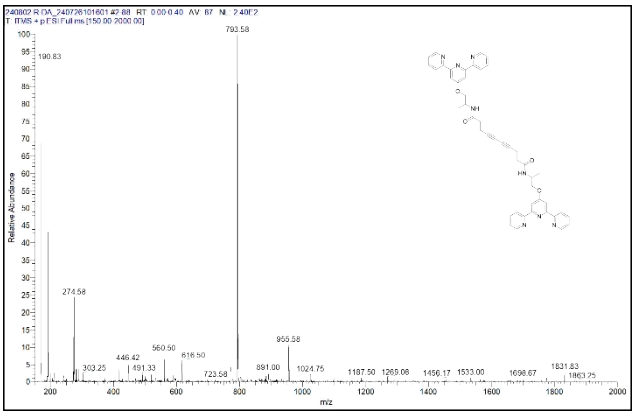

Fig. S28 ESI Mass spectrum of **4** in Methanol.

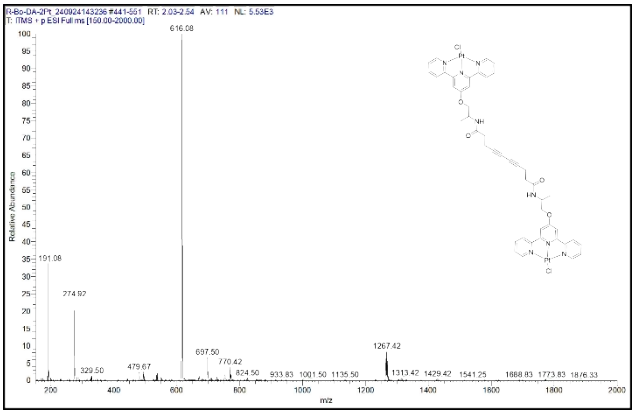

Fig. S29 ESI Mass spectrum of $\mathbf{Pt_2L^1}$ in Methanol.

5. References

1 M. M. J. Smulders, M. M. L. Nieuwenhuizen, T. F. A. de Greef, P. van der Schoot, A. P. H. J. Schenning and E. W. Meijer, *Chem. Eur. J.* 2010, **16**, 362-367.
2 P. Jonkheijm, P. van der Schoot, A. P. H. J. Schenning and E. W. Meijer, *Science,* 2006, **313**, 80-83.
3 A. J. Markvoort, H. M. M. ten Eikelder, P. A. J. Hilbers, T. F. A. de Greef and E. W. Meijer, *Nat. commun.,* 2011, **2**, 509.
4 M. Wehner, M. I. S. Röhr, M. Bühler, V. Stepanenko, W. Wagner and F. Würthner, *J. Am. Chem. Soc.,* 2019, **141**, 6092-6107.
5 S. Dhiman, A. Sarkar and S. J. George, *RSC Adv.,* 2018, **8**, 18913-18925.
6 T. F. A. De Greef, M. M. J. Smulders, M. Wolffs, A. P. H. J. Schenning, R. P. Sijbesma and E. W. Meijer, *Chem. Rev.,* 2009, **109**, 5687-5754.
7 H. M. M. ten Eikelder, A. J. Markvoort, T. F. A. de Greef and P. A. J. Hilbers, *J. Phys. Chem. B.* 2012, **116**, 5291-5301.
8 M. J. Frisch, G. W. Trucks, H. B. Schlegel, G. E. Scuseria, et al., *Gaussian 09*, Gaussian, Inc., Wallingford, CT, **2016**.
9 J. P. Perdew, *Phys. Rev. B*, 1986, **33**, 8822-8824.
10 F. Weigend, *Phys. Chem. Chem. Phys.*, 2006, **8**, 1057-1065.
11 F. Weigend and R. Ahlrichs, *Phys. Chem. Chem. Phys.*, 2005, **7**, 3297-3305.
12 M. Kim, H. Choi, M. Kim, S. Yun, S. Yun, E. Lee, J. Cho, S. H. Jung and J. H. Jung, *Chem. Sci.*, 2024, **15**, 19729-19738.